Non-Radioactive Multiphase Flowmeter for Quantifying Solid Particles Entrained in Fluid Flow

Cornelius Emeka Agu, Evgeniy Tantserev, Arne Tobias Elve, Audun Aspelund

ABBON AS, Baker Østbysvei 5, 1351 Rud, Norway

SUMMARY

Knowledge of solid flow rate or solid fraction in a multiphase flow is essential for management and controlling of the related operational challenges in Oil & Gas companies. For example, the production of sand particles in an aging well can lead to pipeline blockage and erosion. The concentration of drilling cuttings above the threshold may result in poor circulation of drilling fluid. In this paper, ABBON AS proposes an approach by which a non-radioactive multiphase meter can be used to measure the flowrate of solid particles entrained in a fluid flow. The measurement principle and approach proposed are similar to those used in the ABBON 3PM but with additional pressure loss measurement to account for the solid phase loading. To ensure proper splitting of flows into individual rates, this paper also reports the investigation carried out on verification of the response of the impedance sensors under fluid-solid environment using clay particles of density 1855 kg/m^3 and different mean particle sizes, 700, 1200 and 5000 µm. The fluids used in the test include air, oil with permittivity of 2.2 and water with three different salinities in the range, 1 – 15%. The results confirm that both the capacitive and conductive sensors respond appropriately to solids entrained in the fluids, which also agrees with the classical mixing models proposed to use in this metering concept. Furthermore, theoretical error analysis shows that the uncertainties in predicting the mixture density and solid flowrate over the *GVF* range, 1 – 100% lie below ±5% and ±10%, respectively. In a fluid-solid mixture with no gas, the errors can be significantly reduced to 1.5% and 7.5%, respectively.

Keywords: Four-phase meter; MPFM; Non-radioactive meter; ABBON; Drilling solids

1. INTRODUCTION

Worldwide petroleum is largely produced from regions such as Middle East, North Sea and Gulf of Mexico with unconsolidated formations and high sand production potential. As the production wells age, the reservoir strength becomes weaker, thereby leading to production of sand. Sand production can be influenced also by high reservoir fluid viscosity, pore pressure reduction and increase in water cut. Particle depositions associated with sand production can lead to blockage of flowlines, enhanced pipe corrosion as well as increased use of pig traps. These failures can cause unexpected downtime and risk to equipment and personnel. Tracking the concentration of solids in drilling fluid is also essential for service companies to manage drilling operations. Larger amount of solids than

the threshold (usually about 6 – 7% by volume) can lead to high consumption of drilling fluid, reduced drilling rate and poor performance of the overall process.

By continuous measurement of sand production rate, it may be possible to identify potential blockages in the production line. The proper interpretation of the measurements might also predict the critical value of the solid fraction. To enhance this development, multiphase flow meter (MPFM) business is being considered from its conventional use in three-phase systems to applications where up to four phases are involved. Moreover, the complexity of the metering system is a challenge, especially when the fourth phase is solid. The development of MPFM for solid flow measurement is not yet matured and could be difficult when small amount of solids is present in the fluid stream. Today, measurement of the produced solids below the erosion limit is of better interest for oil companies, where any amount as low as early production should be detected [1].

Different studies have been conducted to demonstrate the solid detection potentials in multiphase flow meters based on the gamma ray attenuation, e.g., the Vx technology [1]. Beside the safety related issues with this technology, all traceable studies are limited to solid-liquid-gas three phase systems, which could be due to poor resolution of the third attenuation energy level. Taking the advantage of the non-radioactive meter technology, e.g., the ABBON 3PM, it will be interesting to extend the same to flow systems involving solid phase. The electrical tomography sensors (capacitance and resistance) on which this metering system is based has a number of proven capabilities to measure concentration of solids (no matter the amount) in a given fluid across the cross-section of a pipe [2, 3].

With 17 years of experience, ABBON AS applies advance knowledge and technology in designs of its sensors, signal processing and software development for accurate and reliable measurement of gas, oil and water flowrates. Transferring the same long-proven knowledge and experience, we present herein a comprehensive approach in which a non-radioactive multiphase meter can be used to measure the flow of solid particles entrained in a multiphase fluid. Conventionally, non-radioactive MPFMs combine measurements of fluid mixture conductivity/permittivity, cross correlation velocity and differential pressure across a Venturi throat to predict flow rates of a three-phase flow. When an additional phase is present such as solid particles, a shift in these flow variables will be expected, and thus additional input will be required. For example, with inclusion of water cut or fluid property model as input, the four phase flow rates can be in situ determined. The method proposed in this paper utilizes pressure loss across the meter as the extra input to quantify the fourth phase. To ensure proper splitting of the flow into individual rates, the impedance measurement must be guaranteed. On this basis, this paper also reports the investigation conducted to verify the sensitivity of the impedance sensors to different fluid-solid mixtures at different particle sizes. In the subsequent chapters, the overviews of the ABBON 3PM measurement principle, the method proposed for four-phase flow measurement and the set up used in verifying the impedance sensor sensitivity are given.

2. THREE-PHASE FLOW MEASUREMENT WITH ABBON 3PM

The ABBON three-phase flow meter is based on non-radioactive impedance measurement combined with the fundamental gas-liquid mixing rules to generate the different phase fractions in a multiphase flow. Figure 1 illustrates the structure of the ABBON 3PM, consisting of a long-throated and twin channelled Venturi tube as the primary element; the full description of the meter is reported in [4]. The primary inputs to the meter include the differential pressure, Δp measured between the upstream and the Venturi throat, the fluid impedance, σ_m/ε_m measured withing the throat and the cross-correlation velocity between two impedance signals measured at different locations in the throat. The impedance is correlated with the fraction of cross-sectional area occupied by other phases than gas, where the area fraction of each phase, "*j*" is defined as $\alpha_j = A_j/A$.

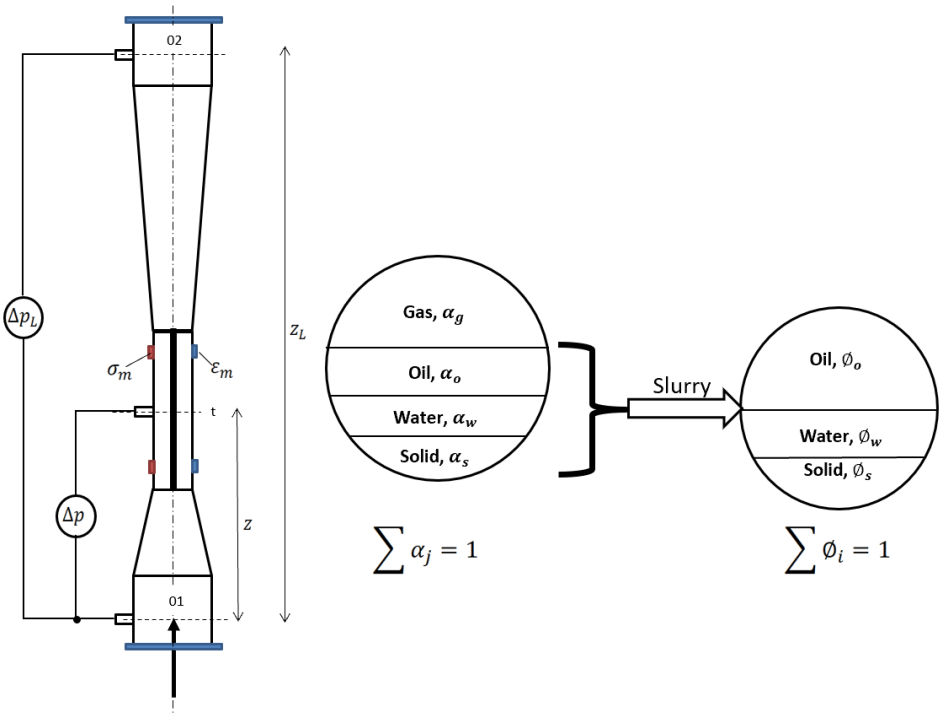

Figure 1. Schematic of the ABBON 3PM showing additional DP sensor for four-phase flow.

The method applied in determining the different phase fractions (excluding the solid phase, "*s*") in the ABBON meter is described by the set of equations, (1) – (4). Equation (1) ensures that the total fraction of the phases is conserved, while Eq. (2) is based on the Bruggeman mixing rules which relates the pure component impedance to the measured fluid mixture impedance, ε_m/σ_m in both oil-continuous (capacitive) and water-continuous (conductive) flows. The expressions for the total mass and volume conservation are represented by Eq. (3). By applying the Bernoulli's principle across points "01" and "t" as indicated in Figure 1, Eq. (4) can be derived for the density of the overall phase mixture. Note that the subscripts "*g*", "*o*", "*w*" and "*m*" denote gas, oil, water and mixture, respectively, and the symbols WLR and S represent water-in liquid ratio and gas-liquid slip ratio, respectively. For a given flow, the mixture velocity, v_m is related to the measured cross-correlation velocity by a mapping function developed in-house by ABBON AS.

Solving the equation set, (1) – (4) simultaneously, the different phase fractions, α_g, α_o and α_w are obtained. The complete set of phase fractions also offers means of splitting the total flow rate into gas, Q_{gas} and liquid, Q_{liq} rates as indicated by Eq. (5) – (7), where GVF is the true gas volume fraction in the total flow.

$$\alpha_g + \alpha_o + \alpha_w = 1 \tag{1a}$$

$$WLR = \frac{\alpha_w}{1-\alpha_g} \tag{1b}$$

$$1 - \alpha_g = \begin{cases} \left(\frac{\varepsilon_m - \varepsilon_g}{\varepsilon_l - \varepsilon_g}\right)\left(\frac{\varepsilon_l}{\varepsilon_m}\right)^{\frac{1}{3}}, & oil - continuous\ flow \\ \left(\frac{\sigma_m}{\sigma_l}\right)^{\frac{2}{3}}, & water - continuous\ flow \end{cases} \tag{2a}$$

$$\varepsilon_l = \frac{\varepsilon_o}{(1-WLR)^3}; \quad \sigma_l = \sigma_w (WLR)^{3/2} \tag{2b}$$

$$\alpha_g S \rho_g + \alpha_o \rho_o + \alpha_w \rho_w = \frac{v_m}{u_l}\rho_m \tag{3a}$$

$$\frac{v_m}{u_l} = \alpha_g S + 1 - \alpha_g \tag{3b}$$

$$\rho_m = \frac{2\Delta p}{\left(\frac{v_m}{C_d}\right)^2 (1-\beta^4) + 2gz} \tag{4}$$

$$GVF = \frac{\alpha_g S}{1+\alpha_g (S-1)} \tag{5}$$

$$Q_{gas} = (GVF) A v_m \tag{6}$$

$$Q_{liq} = (1 - GVF) A v_m \tag{7}$$

Following this measurement principle, the accuracy of the ABBON multiphase flow meter mainly depends on the prediction of the slip ratio, S and the discharge coefficient, C_d as well as the measurement uncertainty of the differential pressure, Δp. By the special function used in the ABBON 3PM, the error in converting the measured cross-corelation to the mixture velocity, v_m is insignificant across the *GVF* (0,1) range. Since the slip ratio is used to map the gas phase fraction, α_g to GVF, the uncertainty in the impedance, ε_m/σ_m measurement is accounted for in the prediction of slip. The ABBON discharge coefficient and slip functions have stable accuracies within 3% and 5%, respectively as shown in Figure 2. Table 1 summarizes the performance of the ABBON 3PM in field applications for measurement of gas rate, liquid rate and *WLR* over the different ranges of *GVF*. Note that the performance of the ABBON meters given in this table is independent of the meter size, flow regime, operating conditions and liquid viscosity as well as the H_2S and CO_2 contents in the gas phase.

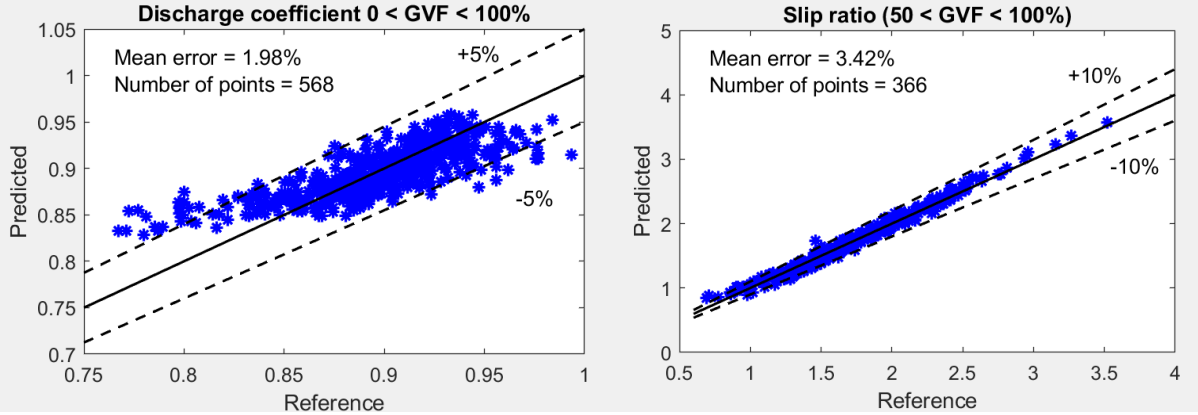

Figure 2. Performance of the discharge coefficient and slip models used in the ABBON 3PM.

Table 1. Range of uncertainties in the ABBON 3PM.

Output variables	Uncertainties		
GVF	0 – 85%	85 – 95%	95 – 98%
Liquid rate (relative)	< 5%	< 5%	< 10%
Gas rate (relative)	< 8%	< 5%	< 5%
WLR (absolute)	< 3%	< 5%	< 10%

3. ABBON PROPOSED METHOD FOR FOUR-PHASE FLOW RATE MEASUREMENT

Solid particles in a fluid flow increases the number of phases expected in a conventional MPFM. To correctly quantify the four phase flowrates, an extra measurement is thus required. In addition to the three primary inputs described above, we propose to use the total pressure loss across the meter as shown in Figure 1 to account for the fourth phase. This means that the physical structure of the proposed four-phase meter will be the same as that of the ABBON 3PM. Since pressure loss in a pipe increases with the fluid mass, Δp_L will be very small when only gas flows through the meter but will increase with increase in the amount of liquid or liquid-solid slurry due to increase in the bulk density. Therefore, the measured pressure loss will be used to predict the bulk density of the liquid-solid slurry which then provides information about the fraction of solid in the slurry based on the known densities of the pure components.

Moreover, the presence of solid particles in a flow can cause a shift in the fluid impedance depending on the electrical property of the particles. While this is the case, it is also expected that the measured impedance at the operating point will lie within the space enveloped by the pure component properties as shown in Figure 3. The principle behind the proposed method for prediction of the fractions of different phases as well as their rates in a four-phase flow system is outlined in the following subsections.

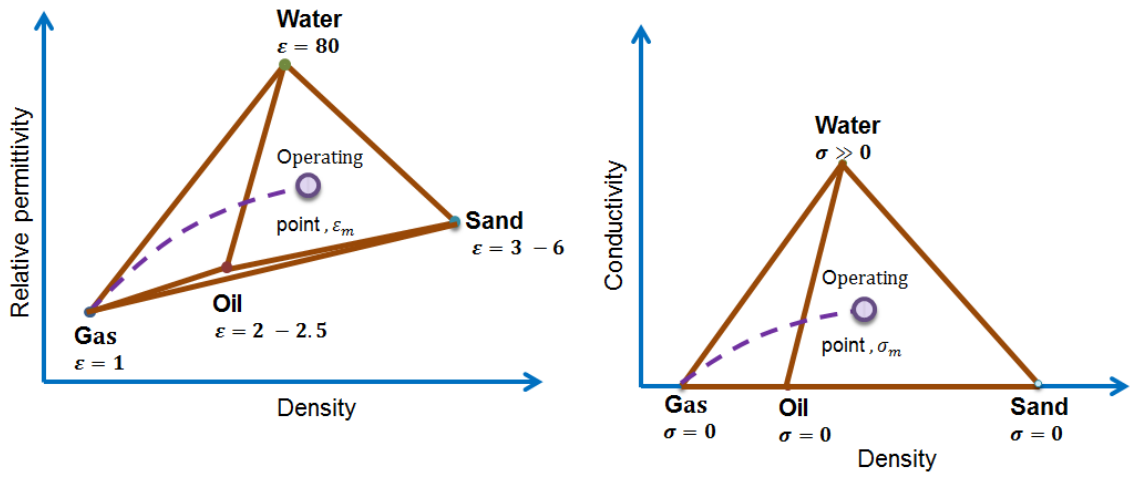

Figure 3. Phase envelope with the operating Impedance in a non-radioactive flow system.

a. Four phase fractions

To relate the solid phase fraction with the measured impedance, a new parameter, $\emptyset_i$ defined as the fraction of area occupied by phase "*i*" in the slurry, is introduced. The slurry phase fraction, $\emptyset_i$ is related to the mixture phase fraction, α_j as expressed in Eq. 8 (a – c). For conservation of different phase fractions, mass and volume, Eq. (9) – (11) are applied. Eq. (12) is derived based on the energy balance (Bernoulli's principle) between points "01" and "02" indicated in Figure 1, and as shown it is applied to predict the density of slurry, ρ_{slurr} in the fluid mixture. The expressions of velocity ratio, v_m/u_l and mixture density, ρ_m are respectively the same as those of Eq. (3b) and (4). While S represents the slip ratio between the gas and slurry phases, the slurry slip ratio, S_s accounts for the differences in the flow velocities between liquid and solid phases.

$$\alpha_o = \emptyset_o(1-\alpha_g) \tag{8a}$$

$$\alpha_w = \emptyset_w(1-\alpha_g) \tag{8b}$$

$$\alpha_s = \emptyset_s(1-\alpha_g) \tag{8c}$$

$$WLR = \frac{\emptyset_w}{1-\emptyset_s} \tag{8d}$$

$$\alpha_g + \alpha_o + \alpha_w + \alpha_s = 1 \tag{9}$$

$$\alpha_g S\rho_g + \alpha_o\rho_o + \alpha_w\rho_w + \alpha_s\rho_s = \frac{v_m}{u_l}\rho_m \tag{10}$$

$$\alpha_o\rho_o + \alpha_w\rho_w + \alpha_s S_s\rho_s = \frac{v_{slurr}}{u_s}(1-\alpha_g)\rho_{slurr} \tag{11a}$$

$$\frac{v_{slurr}}{u_s} = \emptyset_s + S_s(1-\emptyset_s) \tag{11b}$$

$$\rho_{slurr} = \frac{2\Delta p_L}{\left(\frac{v_m}{\beta^2 K}(1-GVF)\right)^2 + 2gz_L} \tag{12}$$

b. Liquid-solid mixing model

Essentially, the fluid impedance is related to the total fraction of non-gas phases in the flow mixture. To accurately apply the Bruggeman mixing formula given by Eq. (13), appropriate mixing rules between the liquid and solid phases are required. Equations (14) and (15) present the mixing models adopted in this proposal for both flow types: oil- and water-continuous flow. The slurry permittivity, ε_{slurr} for non-conductive particles and the slurry conductivity, σ_{slurr} for conductive particles are based on the Maxwell-Garnett and Maxwell-Eucken mixing rules of heterogeneous system, respectively as validated in different literatures [5, 6]. For conductive particles in capacitive flow and non-conductive particles in conductive flow, the expressions of the respective slurry impedance are like those of liquid. The fitting index, m_p depends on the shape of the particles. For a spherical particle, $m_p = 3$ but for a non-spherical particle a larger value close to 4 can be expected [7]. Similarly, the exponent m_c has values in the range 1.8 – 2 for sand-like particles included in a conductive liquid matrix [8].

$$1-\alpha_g = \begin{cases} \left(\frac{\varepsilon_m-\varepsilon_g}{\varepsilon_{slurr}-\varepsilon_g}\right)\left(\frac{\varepsilon_{slurr}}{\varepsilon_m}\right)^{\frac{1}{3}}, & oil-continuous\ flow \\ \left(\frac{\sigma_m}{\sigma_{slurr}}\right)^{\frac{2}{3}}, & water-continuous\ flow \end{cases} \tag{13}$$

$$\varepsilon_{liq} = \varepsilon_o\left(\frac{1}{1-WLR}\right)^3 \tag{14a}$$

$$\varepsilon_{slurr} = \begin{cases} \varepsilon_{liq} + 3\emptyset_s\varepsilon_{liq}\left[\frac{\varepsilon_s-\varepsilon_{liq}}{\varepsilon_s+2\varepsilon_{liq}-\emptyset_s(\varepsilon_s-\varepsilon_{liq})}\right], & Non-conductive\ particles \\ \frac{\varepsilon_{liq}}{(1-\emptyset_s)^{m_p}}, & Conductive\ particles \end{cases} \tag{14b}$$

$$\sigma_{liq} = \sigma_w(WLR)^{\frac{3}{2}} \tag{15a}$$

$$\sigma_{slurr} = \begin{cases} \frac{(1-\emptyset_s)\sigma_{liq}+\emptyset_s\sigma_s\left(\frac{3\sigma_{liq}}{2\sigma_{liq}+\sigma_s}\right)}{(1-\emptyset_s)+\emptyset_s\left(\frac{3\sigma_{liq}}{2\sigma_{liq}+\sigma_s}\right)}, & Conductive\ particles \\ \sigma_{liq}(1-\emptyset_s)^{m_c}, & Non-conductive\ particles \end{cases} \tag{15b}$$

c. Four phase flow rates

From the solution set of Eq. (8) – (15), the respective gas, slurry, liquid and solid flow rates can be obtained using the set of equations, (5), (6) (16) – (19), where $LVFs$ is the true volume fraction of liquid in the slurry. To Split the liquid rate, Q_{liq} into water and oil, the *WLR* computed from Eq. (8d) is applied. In addition to the expected outputs, the different input variables required in the proposed four-phase flow measurement scheme are summarized in Table 2.

$$LVFs = \frac{(1-\emptyset_s)S_s}{\emptyset_s+(1-\emptyset_s)S_s} \tag{16}$$

$$Q_{slurr} = (1-GVF)Av_m \tag{17}$$

$$Q_{liq} = (LVFs)Q_{slurr} \quad (18)$$

$$Q_{sol} = (1 - LVFs)Q_{slurr} \quad (19)$$

Table 2. Required inputs and expected outputs of the proposed ABBON four-phase flowmeter.

Primary inputs	Secondary inputs (references)	Auxiliary inputs	Outputs	
Electrical impedance	Gas specific gravity including CO_2 and H_2S content	Line temperature	Gas flow rate	Q_{gas}
Throat differential pressure	Oil density	Line pressure	Liquid flow rate	Q_{liq}
Pressure loss	Water salinity/density	PVT model	Solid flow rate	Q_{sol}
Cross-correlation velocity	Solid density		Water-liquid ratio/ water cut	WLR, WC
	Oil permittivity		Gas volume fraction/ Gas-oil ratio	GVF, GOR
	Water conductivity		Solid volume fraction	$(1 - LVFs)(1 - GVF)$
	Solid permittivity/ conductivity		Mixture density	ρ_m

4. EFFECT OF SOLID PARTICLES ON FLUID IMPEDANCE

For the proposed four-phase flow measurement method to succeed, the impedance sensors should be able to pick up the changes arising from the ingress of solid particles in the flowing fluid. To verify this, some tests were conducted at the ABBON production hall located at Rud, Norway. The tests were based on clay particles of different size ranges; see Table 3 for the properties of the material. The sensor responses in both conductive and capacitive media were investigated. In the conductive medium, water with different salinities 1, 10 and 15% was used whereas light oil of permittivity of 2.2 was used for the capacitive test. The capacitive sensor was also tested in still air to verify the effect of particle size and size distribution on the permittivity of the solid particles.

The tests were carried out on a static (i.e., no flow) condition with the meter mounted on a bench as shown in Figure 4. The meter was connected to the ABBON flow computer to monitor the response of the sensors. In each of the tests, the particles were gradually fed into the appropriate channel containing the testing sensor. The signals were logged for at least 2 mins over the time before and after the particles were fed in. The results of the tests are presented in Figure 5 and Figure 6.

Table 3. Properties of the solid particles used in the impedance sensitivity test.

Material	Density (kg/m3)	Size range (µm)	Mean size (µm)	Solid fraction (-)	Shape
Dry clay	1855	600 – 850	700	0.397	Angular
Dry clay	1855	1000 – 1400	1200	0.375	Angular
Dry clay	1855	100 – 8000	5000	0.374	Angular

Figure 4. Set up for the impedance sensor sensitivity test around solid particles in fluid phase.

As shown in Figure 5, the different sensors responded appropriately when the particles were introduced. The measured conductivity decreased while the permittivity signals increased as the particles passed through the respective sensors. This pattern of impedance changes in the different media confirms that the clay particles are capacitive with permittivity higher than that of the oil used in the tests. The gradual changes in the impedance signals also indicate that the sensors are sensitivity to different fractions of particles across the measurement cross-section. The figure also shows that the mixture conductivity/permittivity of a given combination of fluid and solid lies within the solution space enveloped by the pure component properties as described in Figure 3.

Figure 6 gives an overview of the effect of particle size and size distribution on the slurry impedance. It can be seen that the higher the particle size, the higher the relative slurry conductivity and the lower the slurry permittivity relative to the liquid permittivity. According to Eq. (14b) and (15b), this means that the sensor readings indicate a decrease in solid fraction as the particle size increases. This behaviour can also be explained by the variation of solid parking density at different sizes, i.e., the solid fraction in a powder decreases with increasing particle size as shown in Table 3. For the same particle size, Figure 6 also shows that the slurry conductivity decreases with increase in the water salinity, which cannot be clearly explained in this paper. Moreover, the pure solid permittivity is independent of the particle size as can be seen from the test with static air.

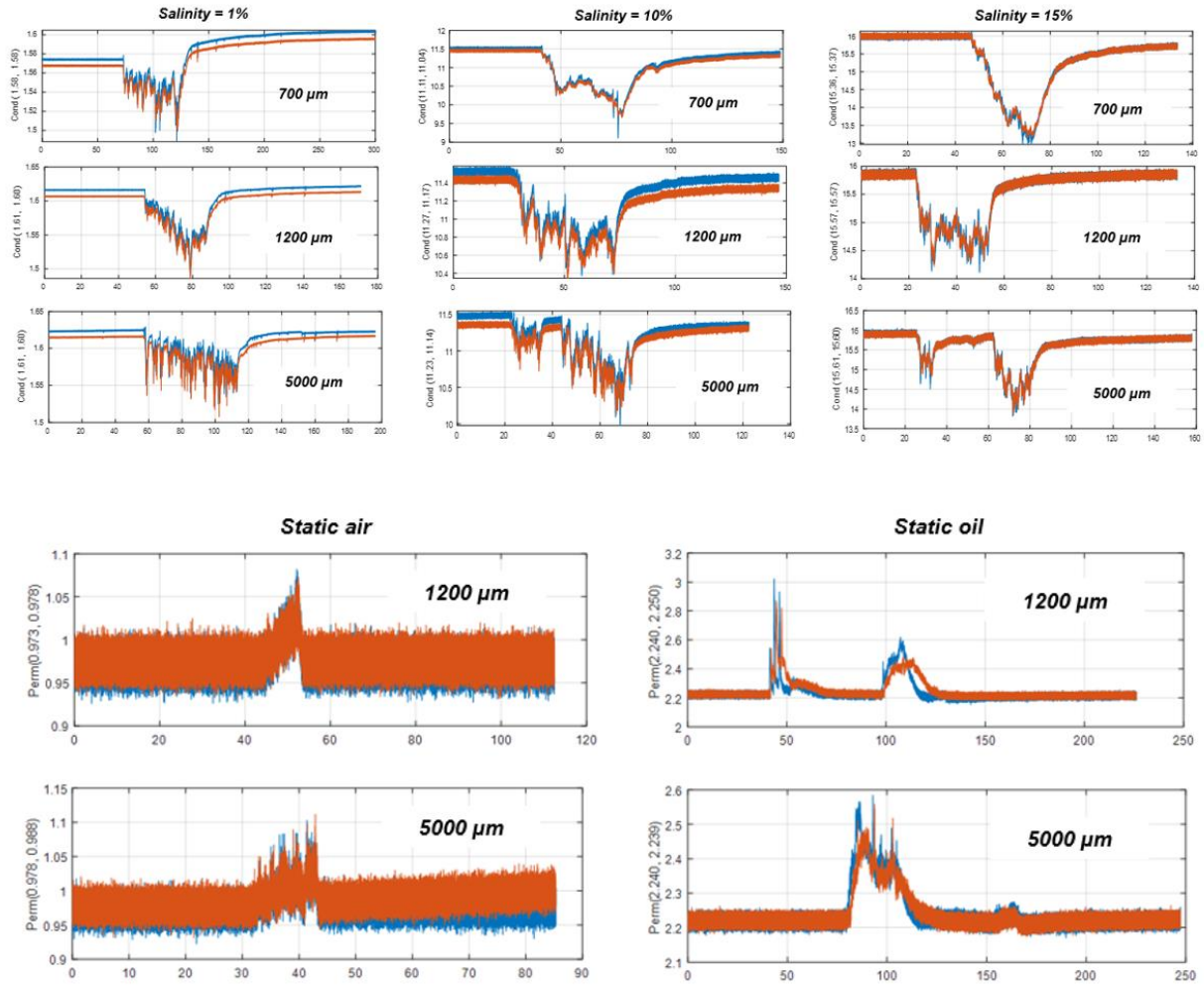

Figure 5. Signals from the conductive and capacitive sensors before, within and after loading of the solid particles with different sizes, where red lines represent the upstream sensor and blue lines the downstream sensor signals.

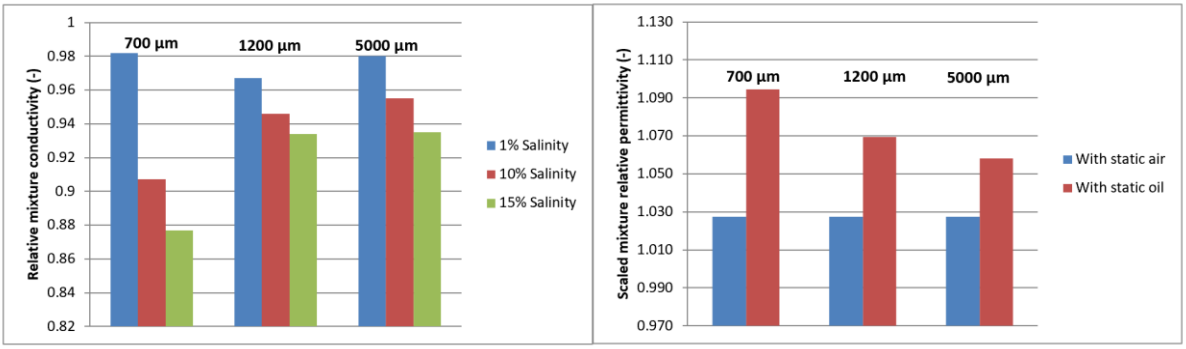

Figure 6. Scaled permittivity and conductivity of the liquid-solid mixture, indicating the effect of particle size on the measurement signals. By the static air test, the relative permittivity of the pure solid particles is independent of the particle size.

5. DISCUSSION

Solid particles entrained in a fluid can cause a proportionate change in the fluid impedance depending on the electrical property of the solid. For the case of clay particles used in the test, there is a positive shift in the relative permittivity of air or oil with addition of the particles. The decrease in water conductivity independent of salinity when the particles are added confirms that the solids are electrically non-conductive. This therefore implies that Eq. (14) and (15) will predict the slurry permittivity and conductivity with reasonable accuracies for a given fraction of solid particles. In the actual flow process, where the four different phases exist, Eq. (13) will then be appropriate to correlate the measured impedance with the pure component properties. For the proposed model to be consistent in predicting the flowrates of the different phases, the gas-slurry slip ratio must be based on the generic definition, Eq. (5) where the gas phase fraction is determined as described above.

The solid particles in a multiphase flow can be combined with the liquid content to form a thick and dense solid-liquid mixture. The slurry may exhibit non-Newtonian behaviour; thus, the usual Newtonian liquid viscosity model may not be valid. Example of how solid particle and size distribution affect the liquid rheology can be found in literature [9]. Since the two model coefficients, C_d and K mainly account for the frictional losses in the flow, the rheology of liquid slurry will be appropriately considered in the correlation of the different coefficients. The Reynolds number used to describe this viscous effect will also be well defined. For non-conductive solid particles, e.g., sand, the phase inversion points between oil- and water-continuous flows may occur at a different *WLR* value than usual. Nevertheless, the transition behaviour will also be considered in the solution of the model.

Though the proposed method is for four-phase flow, a measurement concept based on this principle can also offer accurate readings when the flow involves only one, two or three phases. More accurate results are expected in a liquid-solid or liquid-liquid-solid multiphase flow. In the absence of gas, the method can be used to predict the solid and liquid rates as well as the solid volume fraction and the slurry density independent of the knowledge of the solid density. This aspect is very important in drilling operations where the circulated drilling fluid may contain solids of different densities including the drilling cuttings.

To gain some insights into the potential performance of the proposed measurement method, Eq. (20) – (22) are derived, where ϵ is the uncertainty of the indicated variable. The bulk densities of the overall mixture, slurry and liquid are obtained from Eq. (23) – (25). It should be noted that the uncertainty in the measurement of mixture impedance is lumped into the error in predicting the gas-slurry slip, ϵ_S while the error, ϵ_{S_s} in the slip ratio within the slurry phase also accounts for those expected from the pressure loss, Δp_L measurement and the loss coefficient, K prediction. Figure 7 shows the estimated uncertainties in predicting the mixture density, ϵ_{ρ_m} and the solid volumetric flow rate, $\epsilon_{Q_{sol}}$ for different solid volume fractions. The plots are based on solid density of 2500 kg/m^3, liquid density of 900 kg/m^3 and gas density of 12 kg/m^3. Since DP cells are of high accuracy, $\epsilon_{\Delta p} = 0.5\%$ is assumed. The errors in gas-slurry slip, ϵ_S and discharge coefficient, ϵ_{C_d} are taken as 5% and 3%, respectively as the case in the ABBON 3PM. Because the liquid-solid slip prediction depends on the accuracy of the predicted value of K, the slip error, $\epsilon_{S_s} = 7\%$ is considered. From the plots, the uncertainties in both mixture density and solid rate increase with increasing *GVF* but

with turning points at $GVF \approx 92\%$ and 98%, respectively. With an increase in solid fraction, the error in density prediction increases while that of solid rate decreases. The maximum error over the entire *GVF* range is less than 10% for solid rate and 5% for mixture density. In the drilling operation involving only liquid-solid flow mixture, it will be interesting to see that the proposed method will predict the mixture density with accuracy of ±1.5% and solid rate with accuracy of ±7.5% within the operating range of solid fractions.

$$\epsilon_{\rho_m} = \pm\sqrt{\left\{(1-GVF)\left(\frac{\rho_m-\rho_{slurr}}{\rho_m}\right)\epsilon_S\right\}^2 + \left\{(1-GVF)(1-LVFs)\left(\frac{\rho_{slurr}-\rho_s}{\rho_m}\right)\epsilon_{S_s}\right\}^2} \quad (20)$$

$$\epsilon_{v_m} = \pm\sqrt{{\epsilon_{C_d}}^2 + (0.5\epsilon_{\Delta p})^2 + (0.5\epsilon_{\rho_m})^2} \quad (21)$$

$$\epsilon_{Q_{sol}} = \pm\sqrt{(\epsilon_{S_s}LVFs)^2 + (\epsilon_S GVF)^2 + {\epsilon_{v_m}}^2} \quad (22)$$

$$\rho_m = \rho_g GVF + \rho_{slurr}(1-GVF) \quad (23)$$

$$\rho_{slurr} = \rho_{liq}LVFs + \rho_s(1-LVFs) \quad (24)$$

$$\rho_{liq} = \rho_w WLR + \rho_o(1-WLR) \quad (25)$$

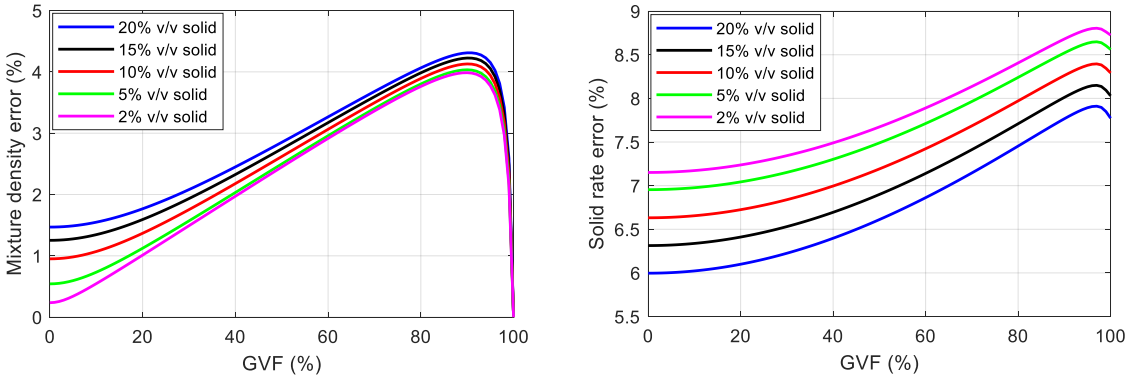

Figure 7. Relative errors in mixture density and solid flow rate as functions of solid and gas volume fractions for 0.5% error, 3% error, 5% error and 7% error in DP measurement and prediction of discharge coefficient, gas-slurry slip and liquid-solid slip ratios, respectively.

6. CONCLUSION

The high accuracy and reliability of the ABBON three-phase flowmeters are traceable to its hardware technology, signal processing technique and enhanced modelling skills of the ABBON R&D team. In this paper, we proposed a measurement principle for four-phase flowrate measurement based on the same physical structure and non-radioactive impedance measurement technology used in the ABBON 3PM. To account for the fourth phase which could be solid, additional inputs such as the total pressure loss across the meter is considered.

The multiphase flowmeter built around this method can accurately be used to monitor the sand production rate for controlling of aging wells, thereby mitigating the adverse effects of flowline

blockage and erosion. In the drilling operations, the multiphase meter can also offer a great benefit in monitoring the solid concentration and providing the density of the return drilling fluid required in the managed pressure drilling system.

The estimated error in the solid rate lies within ±10% and that in the mixture density falls in the range, ±5% over the *GVF* range, 0 – 100%. When the process involves only liquid-solid flow as the case in drilling operations, the errors can be as low as to ±7.5% and ±1.5%, respectively.

Having confirmed that the impedance sensors used in the ABBON meters respond appropriately to the ingress of solid particles, the next step would be to build and test a prototype flowmeter based on the proposed measurement method.

7. SYMBOLS AND ABBREVIATIONS

A	Cross-sectional area [m^2]
C_d	Discharge coefficient [-]
g	Gravity constant [m/s^2]
GOR	Gas-oil ratio [scf/bbl]
GVF	Gas volume fraction [-]
K	Pressure loss coefficient [-]
$LVFs$	Liquid volume fraction in liquid-solid slurry [-]
m_c, m_p	Exponent in liquid-solid mixing model [-]
$\Delta p,\ \Delta p_L$	Pressure drops [Pa]
Q	Volumetric flow rate [m^3/s]
S	Slip ratio [-]
u	Phase velocity [m/s]
v	Bulk/superficial velocity [m/s]
WLR	Water-in-liquid ratio [-]
WC	Water cut [-]
$z,\ z_L$	Elevated height [m]
α	Phase fraction in overall flow mixture [-]
β	Ratio of diameter of the Venturi throat the pipe diameter [-]
ε	Relative permittivity [-]
ϵ	Relative error [%]
σ	Conductivity [S/m]
ρ	Density [kg/m^3]
$\emptyset$	Phase fraction in the liquid-solid slurry [-]

Subscripts

g	Gas
i, j	Phase type
l	Liquid
m	Mixture
o	Oil

s	Solid
w	Water

8. REFERENCES

[1] S. Bifout, B. Pinguet, C. Rojas, How to cope with sand production without any additional sensor when using the right multiphase technology. in: proceedings of the Abu Dhabi International Petroleum Exhibition and Conference, Abu Dhabi, UAE, 10 – 13 November 2014.

[2] C.E. Agu, L.-A. Tokheim, M. Eikeland, B.M.E. Moldestad, Determination of onset of bubbling and slugging in a fluidized bed using a dual-plane electrical capacitance tomography system, Chem. Eng. J. 328 (2017) 997 – 1008.

[3] G. Bolton, S. Stanley, Measurement of solid-liquid mixtures using electrical tomography measurement techniques. in: Proceedings of the 12th International Conference on Environmental Remediation and Radioactive Waste Management, ASME, Volume 1, 2009.

[4] H. Harstad, H.F. Matallah, A. Aspelund, A. Nasri, E. Safar, A. Aburghiba, F.A. Hazeem, M.A. Khatrash, B.A. Ali, F. Samai, A. Khokazian, Field performance evaluation of a non-radioactive MPFM in challenging conditions in the Middle East. in Proceedings of the 35th International North Sea Flow Measurement Workshop, 24 – 26 October 2017.

[5] D.A. Robinson, S.P. Friedman, A method for measuring the solid particle permittivity or electrical conductivity of rocks, sediments, and granular materials, J. Geophys. Res. 108 (2003) 1802 – 1810.

[6] S.M. Zhu, M.R. Zareifard, C.R. Chen, M. Marcotte, S. Grabowski, Electrical conductivity of particle-fluid mixtures in ohmic heating: Measurement and simulation, Food Res. Int. 43 (2010) 1666 – 1672.

[7] K. Lal, R. Parshad, Permittivity of conductor-dielectric heterogeneous mixtures, J. Phys. D: Appl. Phys. 6 (1973) 1788 – 1792.

[8] H. El Khal, A. Cordier, N. Batis, E. Siebert, S. Georges, M.C. Steil, Effect of porosity on the electrical conductivity of LAMOX materials, Solid State Ion. 304 (2017) 75 – 84.

[9] N. Mangesana, R.S. Chikuku, A.N. Mainza, I. Govender, A.P. van der Westhuizen, and M. Narashima, The effect of particle sizes and solids concentration on the rheology of silica sand based suspensions, J. South 108 (2008) 237 – 243.